Analysis of the Seismogenic Activation Potential in the Montney Formation, Northeastern British Columbia and Northwestern Alberta (Parts of NTS 083, 084, 093, 094)

P. Wozniakowska[1], **Department of Geoscience, University of Calgary, Calgary, Alberta, paulina.wozniakowska@ucalgary.ca**

D.W. Eaton, Department of Geoscience, University of Calgary, Calgary, Alberta

Wozniakowska, P. and Eaton, D.W. (2021): Analysis of the seismogenic activation potential in the Montney Formation, northeastern British Columbia and northwestern Alberta (parts of NTS 083, 084, 093, 094); *in* Geoscience BC Summary of Activities 2020: Energy and Water, Geoscience BC, Report 2021-02, p. 81–90.

Introduction

Hydraulic fracturing is used in unconventional resource development to enhance the fluid migration in low-permeability reservoirs. It involves the creation of complex fracture systems during injection of fluids at pressures exceeding in situ breakdown pressures (Smith and Shlyapobersky, 2000). In recent years, hydraulic-fracturing technology has been associated with earthquakes reaching moment magnitudes (M_W) of 5.2 (Lei et al., 2019). Although the basic requirements for generating induced seismicity are well understood (e.g., Ellsworth, 2013; Eaton, 2018), current physical models fail to explain all the fundamental characteristics. One of the extensively studied features is the spatially clustered distribution of induced earthquakes (Skoumal et al., 2015), which has commonly been observed in the Montney Formation (Atkinson et al., 2016; Schultz et al., 2017; Eaton and Schultz, 2018) as well as in other unconventional plays in Canada (Bao and Eaton, 2016; Schultz and Wang, 2020), the United States (Skoumal et al., 2019) and China (Dengfa et al., 2019). Spatial clustering implies a similar underlying distribution of the geological susceptibility to fault activation by hydraulic fracturing.

To date, multiple models have been proposed that seek to explain the physical basis for this apparent variability of geological susceptibility to induced seismicity (Schultz et al., 2016; Shah and Keller, 2017; Pawley et al., 2018). In this study, a machine-learning approach is used to investigate the spatial distribution of the seismogenic activation potential (SAP) in the Montney Formation in British Columbia (BC) and Alberta, where industrial activities have triggered earthquakes of magnitudes as high as M_W 4.6 (Babaie Mahani et al., 2017). The SAP is a probabilistic measure of geological susceptibility to induced earthquake during hydraulic-fracturing operations.

Machine learning has proven to be a helpful tool in many geoscientific areas, including seismic-data processing (Chen et al., 2019), earthquake detection (Perol et al., 2018) and structural interpretation (Huang et al., 2017; Wrona et al.; 2018). Due to its ability to analyze patterns in multidimensional datasets, it can be effectively used to investigate complex relationships and provide additional insights into the mechanisms controlling the occurrence of seismicity induced by hydraulic fracturing (Pawley et al, 2018).

The goal of this study is to reveal underlying mechanisms for seismicity occurring on critically stressed faults in response to elevated pore-fluid pressure. This work is a continuation of the analysis presented in Wozniakowska and Eaton (2020), which investigated the primary factors controlling induced seismicity in the Montney using tree-based algorithms. In the current study, an alternative machine-learning approach (logistic regression) is introduced, the input data and seismicity catalogue are enhanced, and a preliminary seismogenic activation potential map is created for the Montney play.

The project database consisted of 6466 hydraulically fractured horizontal wells and related geological, geomechanical and tectonic characteristics. Each well was classified as seismogenic or nonseismogenic using spatiotemporal association criteria related to seismicity induced by hydraulic fracturing. The next step involved training a supervised machine-learning model to determine the factors controlling the induced seismicity potential in the Montney. In addition, probabilities of seismogenic class determined for each sample were used to estimate the SAP distribution for the whole formation. Based on the results, it appears that seismogenic potential is primarily influenced by the distance to the Cordilleran foreland thrust-and-fold belt and the depth of fractioning-fluid injection. A logistic-regression model predicted the highest occurrence of SAP in the

[1] *The lead author is a 2020 Geoscience BC Scholarship recipient.*

This publication is also available, free of charge, as colour digital files in Adobe Acrobat® PDF format from the Geoscience BC website: http://geosciencebc.com/updates/summary-of-activities/.

a)
b)
c)
British Columbia
Alberta
NPGMMA
KSMMA
Cordilleran TFB
Magnitude (ML)
2.5 - 2.99
3 - 3.49
3.5 - 3.99
4 - 4.49
4.5 - 4.6
Tectonic earthquake
Quarry blast
Induced (Montney)
Induced (not Montney)
Unknown
Seismogenic well
Nonseismogenic well
0 100 200 km
Basement-involved normal fault
Strike-slip fault
Normal fault
Down to basement fault
Dawson Creek graben complex
Phanerozoic thickness [m]
SHmax azimuth [°]
Pressure gradient [kPa/m]
4 7 10 13 16
2000
3000
4000
5000
West
BC
AB
East
Cretaceous
Fernie Fm.
Schooler Creek Gp.
Montney Fm.
Doig Fm.
Belloy Fm.
Stoddart Gp.
Debolt Fm.
Wabamun/Winterburn Gp.
Cambrian
Precambrian
Jurassic
Triassic
Permian
Carboniferous
Devonian
Generalized lithology
Shale
Carbonate
Siltstone
Mixed clastic rocks
Carbonate, clastic and evaporitic rocks
Igneous and metamorphic rocks

Figure 1. The Montney unconventional play (shaded area), showing **a)** seismic magnitude (coloured circles) by category for the period of March 22, 2006 to January 21, 2020, seismogenic (green dots) and nonseismogenic (grey dots) hydraulically fractured horizontal wells drilled into the Montney Formation, the western edge of the Cordilleran foreland thrust-and-fold belt (TFB; dashed line), as well as the North Peace Ground Motion Monitoring Area (NPGMMA) and Kiskatinaw Seismic Monitoring and Mitigation Area (KSMMA) outlined in black (BC Oil and Gas Commission, 2017; Fox and Watson, 2019); **b)** examples of input data used in the study, including maximum horizontal stress (S_{Hmax}) azimuths (Heidbach et al., 2018), Phanerozoic thickness isolines, and known faults influencing the middle and lower units of the Montney (coloured lines) according to type (after Furlong et al., 2020) within the Dawson Creek graben complex; **c)** schematic cross-section through northeastern BC and western Alberta (at about 56°N) of the generalized lithology and age (modified from Liseroudi et al., 2020). Abbreviations: Fm., Formation; Gp., Group.

northwestern part of the Montney, which is consistent with observed seismicity patterns in BC and Alberta (Figure 1a).

Methodology

Input Parameters Description

One of the biggest challenges of machine-learning analysis is data compilation and preprocessing. Incomplete or incorrect information will result in biased predictions. It is important to include all potentially relevant features, as well as potentially insignificant and less obvious characteristics, as the significance (or lack thereof) of each characteristic will be manifested in the feature importance analysis.

The selection of features for this study was dependent on availability of data that could assist in examining current hypotheses concerning the factors influencing SAP distribution in the Montney Formation. As no direct measurements were available for some of the features, proxies were used that were assumed to have a similar correlation with induced seismicity. Interpolated values were used in the case of those features for which no point data were available (see below). Input parameters used in this study and the reasons for their inclusion are presented in Table 1.

Seismicity Data Compilation

Seismicity data (Figure 1a) were compiled from publicly available catalogues provided by Natural Resources Canada (Visser et al., 2017; Huang et al., 2020; Visser et al., 2020), Alberta Energy Regulator (https://ags-aer.maps.arcgis.com) and Canadian Induced Seismicity Collaboration (Cui et al., 2015). The final catalogue included the events from the period between January 1, 2006 and January 21, 2020. The spatial and temporal variability of the magnitude of completeness was investigated to determine the threshold of the seismicity that would guarantee unbiased classification of hydraulically fractured wells. Magnitude of completeness for the 2006–2013 period ranged from local magnitude (M_L) = 2.0 for southwestern Alberta to M_L 3.0 in the northeastern corner of Alberta (Stern et al., 2013; Schultz et al., 2015; Cui and Atkinson, 2016). More recent catalogues (2014–2016) are estimated to have a magnitude of completeness of M_L = 1.8 (northeastern BC and western Alberta), whereas the rest of the Western Canada Sedimentary Basin was estimated at M_L~2.3. Considering the detectability thresholds throughout the entire period, only earthquakes above M_L 2.5 were considered for this analysis; the threshold was based on the local magnitude (M_L), which was the primary magnitude scale used for the compiled seismic catalogues. Natural earthquakes and seismicity associated with industrial activities other than hydraulic fracturing in the Montney were removed from the analysis. Data removed included quarry blasts (Dokht et al., 2020), saltwater disposal wells and hydraulic fracturing in other unconventional plays, including the Duvernay Formation (Schultz et al., 2017; Eaton and Schultz, 2018), and drilling activity in the Horn River Basin (BC Oil and Gas Commission, 2012; Farahbod et al., 2015).

Well Labels

A spatiotemporal association filter was implemented to label wells as seismogenic or nonseismogenic. Following previously published studies that investigated induced seismicity in western Canada (e.g., Atkinson et al., 2016), wells were identified as seismogenic if one (or more) induced earthquakes above M_L 2.5 had occurred after the start of hydraulic-fracturing operations (to establish potential causality) and within three months after operations were completed (the maximum estimated lag time). To address the uncertainty of earthquake location, a spatial constraint was applied specifying that the event epicentre had to be located within 5 km of the horizontal wellbore.

Data Preprocessing and Model Development

Feature Interpolation

The compilation of features for machine-learning analysis required interpolation of irregularly sampled input data. Data-point values, such as formation tops, pressure and maximum horizontal-stress values, were interpolated to determine the values corresponding to each of the wells, which were then inspected to ensure that valid interpolated values had been obtained. For example, data were analyzed to ensure correct stratigraphic association (Montney Formation – Debolt Formation – Precambrian basement), depth of the hydraulic-fracturing operation (approximated by the true vertical depth of the well) within the Montney Formation, as well as depth-index values (correct values are indicated by depth index ranging between 0 and 1; Table 1). Erroneous wells were excluded from further analysis. Only horizontal wells were considered, as production had ended at nearly all Montney vertical wells before the start of this analysis. The final dataset consisted of 6466 hydraulically fractured wells spread over a significant area of

Table 1. Description of the input parameters used in the analysis of the seismogenic activation potential in the Montney Formation.

Characteristic	Background
Distance to the Cordilleran deformation front	Distance from the deformation front is used here as a proxy for tectonic strain (Kao et al., 2018).
Injection depth	Injection depth is used here as a proxy for the target-formation depth, documented to strongly correlate with probability of induced seismicity (Ries et al., 2020).
Vertical distance to top of Precambrian basement	Previous studies suggest higher susceptibility in the vicinity of crystalline basement (Hincks et al., 2018; Kozłowska et al., 2018; Skoumal et al., 2018).
Pore-pressure gradient	A correlation between induced seismicity and formation overpressure has been identified by Eaton and Schultz (2018) and Ries et al. (2020).
Difference between local and regional average S_{Hmax} direction	Rotation of maximum horizontal-stress direction (S_{Hmax}) may be indicative of nearby critically stressed fault (McLellan et al., 2014; Zhang et al., 2019).
Vertical distance to Debolt Formation	This massive carbonate unit is documented to host larger magnitude induced seismicity (Riazi et al., 2020).
Depth index (fractional depth from top to base of Montney)	Completions in the lower and middle units of the Montney appear to be more prone to induce seismicity compared to those in the upper and middle units (BC Oil and Gas Commission, 2014).
Distance to the closest (known) fault	Virtually all currently existing models for seismicity induced by hydraulic fracturing assume that slip occurs on a pre-existing fault (Eaton, 2018).

the study region (Figure 1a). Part of the machine-learning process involved randomly splitting the total number of wells into a training set (including labeled samples, used to determine the model coefficients) and a testing set (including unlabeled samples, used to evaluate the performance of the model; James et al., 2013). Implementing a standard train-test split ratio (75:25) resulted in 4849 samples being assigned to the training set and 1617 samples to the testing set.

Logistic Regression

Logistic regression is a type of supervised machine learning (James et al., 2013); for an *n*-dimensional problem the classification probability p is given by

$$p = 1/\left(1 + e^{-\left[\beta_0 + \beta_1 * x_1 + \ldots + \beta_n * x_n\right]}\right) \quad (1)$$

where x_i, $i = 1,\ldots 7$, are the normalized input-data values at each well location and the parameter weights β_i are calculated during the training phase. Probabilities calculated for each well and coefficients of the model were obtained by averaging individual realizations over 1000 bootstrap samples. Wells with $p > 0.5$ are labelled as seismogenic, whereas samples with lower probabilities correspond to nonseismogenic wells.

Results

Feature Importance Analysis

Feature importance was investigated using the weights extracted from the trained logistic-regression model. The algorithm was developed using scikit-learn, a Python library for machine learning. Ultimate feature weights correspond to average weights of the normalized input parameters from the multiple bootstrap realizations (Equation 1). The values of the model coefficients are indicative of the relative influence of each parameter on the classification results (Molnar, 2019). Based on this analysis, distance to the Cordilleran foreland thrust-and-fold belt and depth of the hydraulic-fracturing operation are the two most important characteristics controlling the SAP. The vertical distance to the top of the Precambrian basement, the difference between local and regional S_{Hmax} and the pore-pressure gradient are moderately important. Remaining parameters (i.e., vertical distance to the Debolt Formation, depth index and distance to known faults) have no influence on SAP distribution (Figure 2a).

SAP Distribution Map

A map of the SAP distribution was created based on the probability of the seismogenic class for each hydraulically fractured well; probabilities were interpolated using a radial-basis function (Lazzaro and Montefusco, 2002). The extrapolation outside the location of the wells over the regular grid yielded values beyond the [0,1] range; therefore, normalization was done to obtain the values matching the realistic probability values (Figure 3). Virtually all higher magnitude (M_L =2.5) earthquakes induced by hydraulic fracturing occurred within the Kiskatinaw Seismic Monitoring and Mitigation Area (KSMMA) and the North Peace Ground Motion Monitoring Area (NPGMMA); both seis-

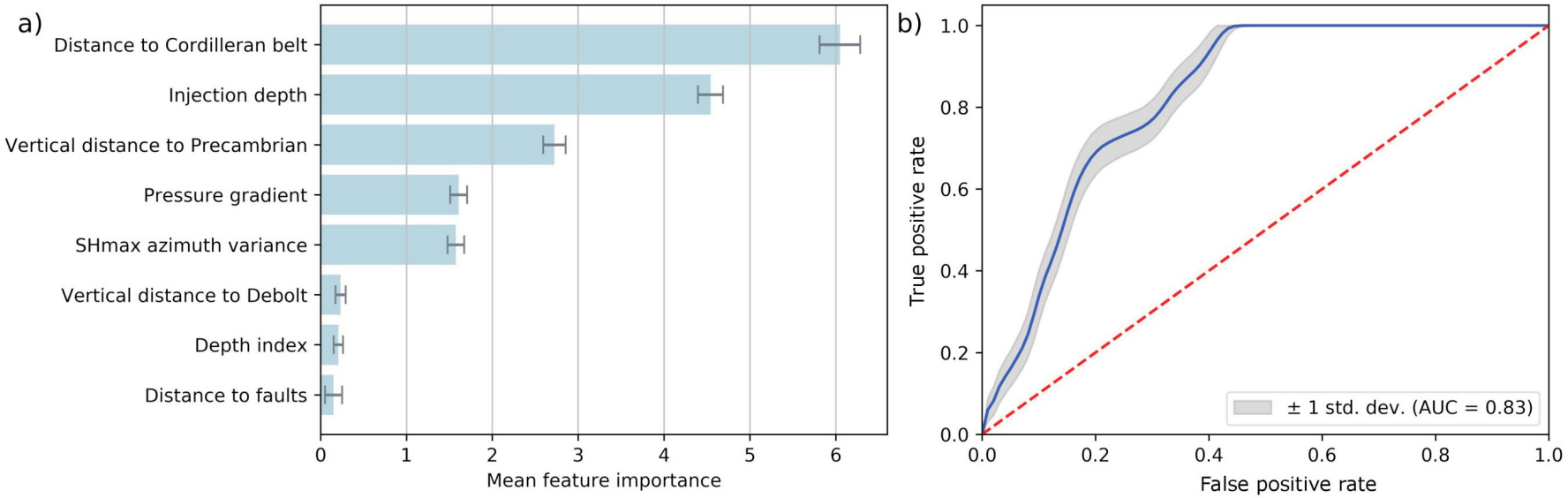

Figure 2. a) Logistic-regression model coefficients. **b)** Average receiver operating characteristic (ROC) curve calculated using 1000 stratified random shuffles (shaded area represents one standard deviation). Abbreviations: AUC, area under the ROC curve; Debolt, Debolt Formation; std. dev., standard deviation.

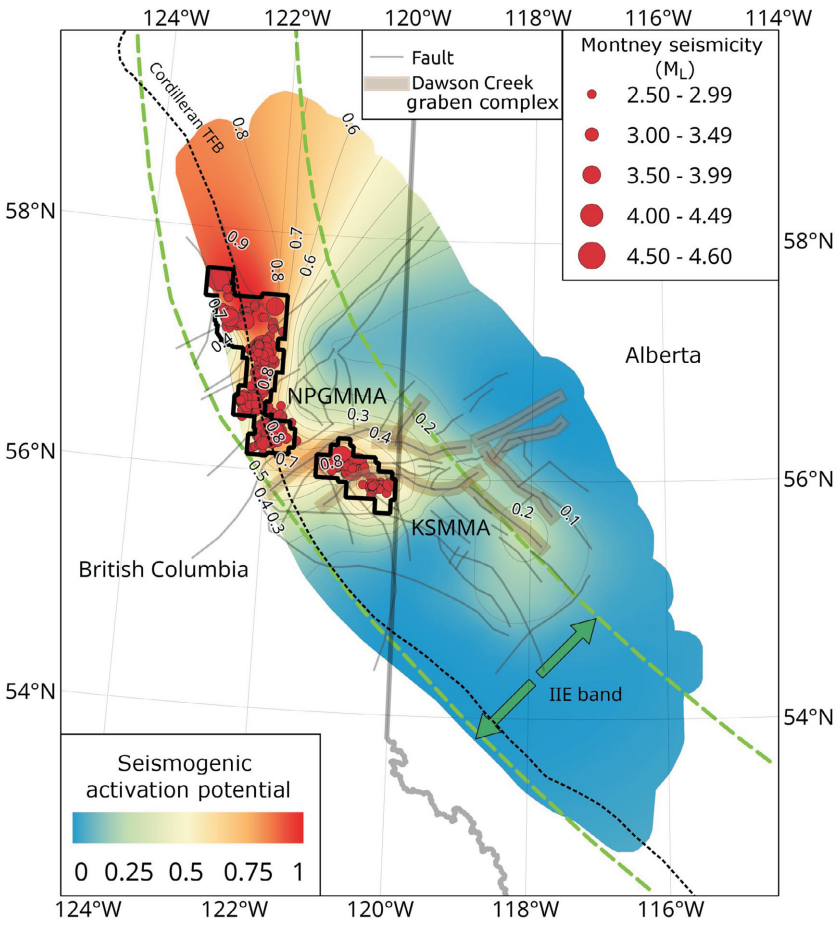

Figure 3. Seismogenic activation potential (SAP) in the Montney Formation. The red circles indicate local magnitude (M_L) =2.5 seismic events associated with hydraulic fracturing in the Montney Formation. Black outlines correspond to seismicity monitoring areas. Approximate range of the injection-induced earthquake (IIE) band is marked by the green dashed lines (after Kao et al., 2018). Cordilleran foreland thrust-and-fold belt (TFB; black dashed line), known faults and Dawson Creek graben complex are also shown. Abbreviations: KSMMA, Kiskatinaw Seismic Monitoring and Mitigation Area; NPGMMA, North Peace Ground Motion Monitoring Area.

micity monitoring areas correspond to areas of higher seismogenic potential (SAP > 0.5; Figure 3).

The highest SAP values (>0.8) are located north of the NPGMMA in BC, whereas the KSMMA region is characterized by a slightly lower SAP, reaching ~0.8 only in its western part. Within Alberta, the SAP of the Montney does not exceed 0.5, excluding a small portion in its northern part, where no hydraulic fracturing operations have yet taken place.

Performance Evaluation

Performance of the machine-learning algorithm was evaluated using the receiver operating characteristics (ROC) curve, which plots the true positive rate versus the false positive rate (Figure 2b) for the validation dataset (Davis and Goadrich, 2006). The area under the ROC curve of the logistic-regression model achieved a score of 0.83, as compared to a value of 0.5 corresponding to the accuracy of random guesses. However, this study is an example of unbalanced classification, characterized by an unequal ratio between samples in one of the specific classes (majority of wells are nonseismogenic). Therefore, metrics other than the ROC may be more suitable to evaluate the performance of the predictive model (Saito and Rehmsmeier, 2015). Hence, the 'recall' score was computed, as it may be better suited to induced-seismicity classification since it quantifies the correct positive class predictions (correctly predicted seismogenic wells) relative to the all positive predictions (both correctly and incorrectly predicted seismogenic wells). 'Recall' is defined as

Recall = true positives/(true positives + false negatives)

The study model achieved a recall score of 77.92%, which provides a good indication that the approach was successful.

Discussion

The results of this study can be compared with those of recent studies that investigated the seismogenic potential in other unconventional plays. It is important to note that choice of input parameters strictly depends on the availability of data and the geological setting of the specific region. Despite the differences in the input features, individual trends can be used to determine the major parameters influencing the induced-seismicity potential in each of the unconventional plays.

For example, Pawley et al. (2018) used a similar machine-learning technique to investigate the SAP distribution in the Duvernay Formation. Their analysis revealed that seismogenic potential in the Duvernay play is influenced by the vertical proximity to the crystalline basement, formation overpressure and minimum horizontal-stress value. In the model developed for this study, distance to the Precambrian basement was shown to be less important than the distance to the Cordilleran foreland thrust-and-fold belt and the depth of hydraulic-fracturing operations.

In contrast to the commonly established mechanisms regarding induced seismicity on pre-existing faults (Eaton, 2018), influence of the known fault structures is not supported by any of these models. Specifically, the distance to known faults both in the Montney and the Duvernay formations was indicated as one of the least important features. Information about the location, type and stress state of the faults in the area is inferred to likely be incomplete. Other geological proxies can be used to infer the potential location of unmapped faults. For example, the presence of lithium-rich brines can be indicative of the faults acting as hydrogeological pathways connecting upper sedimentary layers with the Precambrian basement (Pawley at al., 2018). Further work is needed to obtain lithium-concentration data throughout the Montney play.

As noted above, distance to the western edge of the Cordillera emerges as the most important factor controlling the distribution of SAP in the Montney. This appears to be consistent, at least in part, with the hypothesis of Kao et al. (2018) regarding the correlation of SAP with areas showing an elevated rate of tectonic strain. However, this association does not explain the apparent difference in seismicity levels for Montney wells located at an equivalent distance from the deformation front in BC and Alberta.

Conclusions and Future Work

In this study, a machine-learning approach was used to investigate the spatial variability of induced seismicity in the Montney Formation during hydraulic-fracturing operations. Areas with higher values of the calculated SAP are congruent with the observed pattern of induced seismicity. The map (Figure 3) indicates lower SAP values for the Montney in Alberta, which is consistent with seismicity observations. Multiple hypotheses were tested regarding the factors controlling the potential of fault-slip activation during hydraulic fracturing. The model shows that SAP in the Montney play is primarily controlled by proximity to the Cordilleran deformation front and the depth of fluid injection during hydraulic-fracturing operations. The area of highest SAP (>80%) occurs in the northwestern part of the subsurface extent of the Montney Formation, which is outside both the KSMMA and NPGMMA seismic monitoring regions. Planned future research will include incorporation of new input parameters and enhancement of key sources of data currently being used. More complete information about the distribution and stress state of the faults in the area, the influence of operational parameters and the distinctions between events triggered by completions performed in the upper, middle and lower units of the Montney present some of the current limitations that need to be addressed to better understand the complex mechanisms driving seismicity induced by hydraulic fracturing in the Montney Formation.

Acknowledgments

Geoscience BC and sponsors of the Microseismic Industry Consortium are thanked for their financial support of this research. The authors also thank geoLOGIC systems ltd. for providing access to compiled proprietary and public data used in this study. They are also grateful to C. Furlong for her comments that helped to improve this manuscript.

References

Atkinson, G.M., Eaton, D.W., Ghofrani, H., Walker, D., Cheadle, B., Schultz, R., Shcherbakov, R., Tiampo, K., Gu, J., Harrington, R.M. and Liu, Y. (2016): Hydraulic fracturing and seismicity in the Western Canada Sedimentary Basin; Seismological Research Letters, v. 87, no. 3, p. 631–647, URL <https://www.inducedseismicity.ca/wp-content/uploads/2015/01/r16_Atkinson-et-al_Hydraulic-Fracturing-and-Seismicity-in-the-Western-Canada-Sedimentary-Basin.pdf> [March 2016].

Babaie Mahani, A., Schultz, R., Kao, H., Walker, D., Johnson, J. and Salas, C. (2017): Fluid injection and seismic activity in the northern Montney play, British Columbia, Canada, with special reference to the 17 August 2015 M_W 4.6 induced earthquake; Bulletin of the Seismological Society of America, v. 107, no. 2, p. 542–552, URL <https://www.ernstversusencana.ca/wp-content/uploads/2017-April-Mahani-et-al-Fluid-injection-seismic-Activity-in-N-Monteney-Play-BC-w-special-ref-to-Aug-17-2005-4.6M-induced-earthquake.pdf> [February 2017].

Bao, X. and Eaton, D.W. (2016): Fault activation by hydraulic fracturing in western Canada; Science, v. 354, no. 6318, p. 1406–1409, URL <https://science.sciencemag.org/content/354/6318/1406> [December 2016].

BC Oil and Gas Commission (2012): Investigation of observed seismicity in the Horn River Basin; BC Oil and Gas Commission, Technical Report, 29 p., URL <http://www.bcogc.ca/node/8046/download> [August 2012].

BC Oil and Gas Commission (2014): Investigation of observed seismicity in the Montney Trend; BC Oil and Gas Commission, Technical Report, 32 p., URL <https://www.bcogc.ca/files/reports/Technical-Reports/investigation-observed-seismicity-montney-trend.pdf> [December 2014].

BC Oil and Gas Commission (2017): Guidance for ground motion monitoring and submission; BC Oil and Gas Commission, 2 p., URL <https://www.bcogc.ca/files/operations-documentation/Induced-Seismicity-Data-and-Submission/ground-motion-guidance-document-december-20-release-2017.pdf> [December 2017].

Chen, Y., Zhang, M., Bai, M. and Chen, W. (2019): Improving the signal-to-noise ratio of seismological datasets by unsupervised machine learning; Seismological Research Letters, v. 90, no. 4, p. 1552–1564, URL <https://www.seismosoc.org/wp-content/uploads/2019/07/SRL-90.3-Machine-Learning.pdf> [July 2019].

Cui, L. and Atkinson, G.M. (2016): Spatiotemporal variations in the completeness magnitude of the Composite Alberta Seismicity Catalog (CASC); Seismological Research Letters, v. 87, no. 4, p. 853–863, URL <https://doi.org/10.1785/0220150268>.

Cui, L., Fereidoni, A. and Atkinson, G.M. (2015): Compilation of Composite Alberta Seismicity Catalog (CASC) for earthquake hazard from induced seismicity in Alberta; American Geophysical Union–Geological Association of Canada–Mineralogical Association of Canada–Canadian Geophysical Union, Joint Assembly, May 3–7, 2015, Montréal, Québec, poster presentation, URL <https://www.inducedseismicity.ca/wp-content/uploads/2015/01/AlbertaCompCat2020-01-1.zip> [November 2015].

Davis, J. and Goadrich, M. (2006): The relationship between Precision-Recall and ROC curves; *in* Proceedings of the 23rd International Conference on Machine Learning, W. Cohen and A. Moore (ed.), June 25–29, 2006, Pittsburgh, Pennsylvania, p. 233–240, URL <https://doi.org/10.1145/1143844.1143874>.

Dengfa, H.E., Renqi, L.U., Huang, H., Xiaoshan, W., Jiang, H. and Zhang, W. (2019): Tectonic and geological setting of the earthquake hazards in the Changning shale gas development zone, Sichuan Basin, SW China; Petroleum Exploration and Development, v. 46, no. 5, p. 1051–1064, URL <https://www.sciencedirect.com/science/article/pii/S187638041960262?via%3Dihub> [October 2019].

Dokht, R.M., Smith, B., Kao, H., Visser, R. and Hutchinson, J. (2020): Reactivation of an intraplate fault by mine-blasting events: implications to regional seismic hazard in Western Canada; Journal of Geophysical Research: Solid Earth, v. 125, no. 6, art. e2020JB019933, URL <https://doi.org/10.1029/2020JB019933>.

Eaton, D.W. (2018): Passive seismic monitoring of induced seismicity: fundamental principles and application to energy technologies; Cambridge University Press, Cambridge, United Kingdom, 360 p.

Eaton, D.W. and Schultz, R. (2018): Increased likelihood of induced seismicity in highly overpressured shale formations; Geophysical Journal International, v. 214, no. 1, p. 751–757, URL <https://www.inducedseismicity.ca/wp-content/uploads/2015/01/r18_Eaton-and-Schultz_Increased-likelihood-of-IS-in-highly-overpressured-shale-formations.pdf> [July 2018].

Ellsworth, W.L. (2013): Injection-induced earthquakes; Science, v. 341, no. 6142, 7 p., URL <https://science.sciencemag.org/content/341/6142/1225942> [July 2013].

Farahbod, A.M., Kao, H., Walker, D.M. and Cassidy, J.F. (2015): Investigation of regional seismicity before and after hydraulic fracturing in the Horn River Basin, northeast British Columbia; Canadian Journal of Earth Sciences, v. 52, no. 2, p. 112–122, URL <https://doi.org/10.1139/cjes-2014-0162>.

Fox, A.D. and Watson, N.D. (2019): Induced seismicity study in the Kiskatinaw Seismic Monitoring and Mitigation Area, British Columbia; report prepared by Enlighten Geoscience Ltd. for the BC Oil and Gas Commission, 51 p., URL <https://www.bcogc.ca/files/reports/Technical-Reports/final-report-enlighten-geoscience-kssma-phase-1-study-2019w-appendices-links.pdf> [June 2019].

Furlong, C.M., Gingras, M.K. and Zonneveld, J.P. (2020): High-resolution sequence stratigraphy of the Middle Triassic Sunset Prairie Formation, Western Canada Sedimentary Basin, north-eastern British Columbia; The Depositional Record, v. 6, no. 2, p. 383–408, URL <https://doi.org/10.1002/dep2.107>.

Heidbach, O., Rajabi, M., Cui, X., Fuchs, K., Müller, B., Reinecker, J., Reiter, K., Tingay, M., Wenzel, F., Xie, F., Ziegler, M.O., Zoback, M.-L. and Zoback, M. (2018): The World Stress Map database release 2016: crustal stress pattern across scales; Tectonophysics, v. 744, p. 484–498, URL <https://doi.org/10.1016/j.tecto.2018.07.007>.

Hincks, T., Aspinall, W., Cooke, R. and Gernon, T. (2018): Oklahoma's induced seismicity strongly linked to wastewater injection depth; Science, v. 359, no. 6381, p. 1251–1255, URL <https://science.sciencemag.org/content/359/6381/1251.full> [March 2018].

Huang, L., Dong, X. and Clee, T.E. (2017): A scalable deep learning platform for identifying geologic features from seismic attributes; The Leading Edge, v. 36, no. 3, p. 249–256, URL <https://doi.org/10.1190/tle36030249.1>.

Huang, G.D., Kao, H. and Gu, Y.J. (2020): A comprehensive earthquake catalogue for southwestern Alberta, between 2004 and 2015; Geological Survey of Canada, Open File 8705, 49 p., URL <https://doi.org/10.4095/321826>.

James, G., Witten, D., Hastie, T. and Tibshirani, R. (2013): An introduction to statistical learning – with applications in R; Springer-Verlag, New York, New York, 426 p., URL<https://doi.org/10.1007/978-1-4614-7138-7>.

Kao, H., Hyndman, R., Jiang, Y., Visser, R., Smith, B., Babaie Mahani, A., Leonard, L., Ghofrani, H. and He, J. (2018): Induced seismicity in western Canada linked to tectonic strain rate: implications for regional seismic hazard; Geophysical Research Letters, v. 45, no. 20, p. 11 104–11 115, URL <https://doi.org/10.1029/2018GL079288>.

Kozłowska, M., Brudzinski, M.R., Friberg, P., Skoumal, R.J., Baxter, N.D. and Currie, B.S. (2018): Maturity of nearby faults influences seismic hazard from hydraulic fracturing; Proceedings of the National Academy of Sciences, v. 115, no. 8, p. E1720–E1729, URL <https://www.pnas.org/content/115/8/E1720> [February 2018].

Lazzaro, D. and Montefusco, L.B. (2002): Radial basis functions for the multivariate interpolation of large scattered data sets; Journal of Computational and Applied Mathematics, v. 140, no. 1–2, p. 521–536, URL <https://core.ac.uk/download/pdf/82502771.pdf> [September 2000].

Lei, X., Wang, Z. and Su, J. (2019): The December 2018 M_L 5.7 and January 2019 M_L 5.3 earthquakes in South Sichuan Basin induced by shale gas hydraulic fracturing; Seismological Research Letters, v. 90, no. 3, p. 1099–1110, URL <https://pubs.geoscienceworld.org/ssa/srl/article-abstract/90/3/1099/569798/The-December-2018-ML-5-7-and-January-2019-ML-5-3?redirectedFrom=fulltext> [April 2019].

Liseroudi, M.H., Ardakani, O.H., Sanei, H., Pedersen, P.K., Stern, R.A. and Wood, J.M. (2020): Origin of sulfate-rich fluids in the Early Triassic Montney Formation, Western Canadian Sedimentary Basin; Marine and Petroleum Geology, v. 114, art. 104236, URL <https://doi.org/10.1016/j.marpetgeo.2020.104236>.

McLellan, P., Anderson, I., Wong, J. and Mostafavi, V. (2014): Geomechanical characterization of the Farrell Creek Montney reservoir, northeast British Columbia; GeoConvention 2014, Canadian Society of Petroleum Geologists-Canadian Society of Exploration Geophysicists-Canadian Well Logging Society, Joint Annual Convention, May 12–16, 2014, Calgary, Alberta, extended abstract, 2 p., URL <https://www.researchgate.net/publication/313879972_Geomechanical_Characterization_of_the_Farrell_Creek_Montney_Reservoir_Northeast_British_Columbia> [May 2014].

Molnar, C. (2019): Interpretable machine learning – a guide for making black box models explainable; Lulu, 318 p., URL <https://christophm.github.io/interpretable-ml-book/> [November 2020].

Pawley, S., Schultz, R., Playter, T., Corlett, H., Shipman, T., Lyster, S. and Hauck, T. (2018): The geological susceptibility of induced earthquakes in the Duvernay play; Geophysical Research Letters, v. 45, no. 4, p. 1786–1793, URL <https://doi.org/10.1002/2017GL076100>.

Perol, T., Gharbi, M. and Denolle, M. (2018): Convolutional neural network for earthquake detection and location; Science Advances, v. 4, no. 2, art. e1700578, URL <https://doi.org/10.1126/sciadv.1700578>.

Riazi, N., Eaton, D.W., Aklilu, A. and Poulin, A. (2020): Application of focal-time analysis for improved induced seismicity depth control: a case study from the Montney Formation, British Columbia, Canada; Geophysics, v. 85, no. 6, p. 1–70, URL <https://prism.ucalgary.ca/handle/1880/112701> [October 2020].

Ries, R., Brudzinski, M.R., Skoumal, R.J. and Currie, B.S. (2020): Factors influencing the probability of hydraulic fracturing-induced seismicity in Oklahoma; Bulletin of the Seismological Society of America, v. 110, no. 5, p. 2272–2282, URL <https://doi.org/10.1785/0120200105>.

Saito, T. and Rehmsmeier, M. (2015): The precision-recall plot is more informative than the ROC plot when evaluating binary classifiers on imbalanced datasets; PloS ONE, v. 10, no. 3, 21 p., URL <https://doi.org/10.1371/journal.pone.0118432>.

Schultz, R. and Wang, R. (2020): Newly emerging cases of hydraulic fracturing induced seismicity in the Duvernay East Shale Basin; Tectonophysics, v. 779, art. 228393, URL <https://doi.org/10.1016/j.tecto.2020.228393>.

Schultz, R., Corlett, H., Haug, K., Kocon, K., MacCormack, K., Stern, V. and Shipman, T. (2016): Linking fossil reefs with earthquakes: geologic insight to where induced seismicity occurs in Alberta; Geophysical Research Letters, v. 43, no. 6, p. 2534–2542, URL <https://doi.org/10.1002/2015GL067514>.

Schultz, R., Stern, V., Gu, Y.J. and Eaton, D. (2015): Detection threshold and location resolution of the Alberta Geological Survey earthquake catalogue; Seismological Research Letters, v. 86, no. 2A, p. 385–397, URL <https://pdfs.semanticscholar.org/c58e/0f16df77818121d11a9c1128b79e99dd38aa.pdf> [September 2020].

Schultz, R., Wang, R., Gu, Y.J., Haug, K. and Atkinson, G.M. (2017): A seismological overview of the induced earthquakes in the Duvernay play near Fox Creek, Alberta; Journal of Geophysical Research: Solid Earth, v. 122, no. 1, p. 492–505, URL <https://doi.org/10.1002/2016JB013570>.

Shah, A.K. and Keller, G.R. (2017): Geologic influence on induced seismicity: constraints from potential field data in Oklahoma; Geophysical Research Letters, v. 44, no. 1, p. 152–161, URL <https://doi.org/10.1002/2016GL071808>.

Skoumal, R.J., Brudzinski, M.R. and Currie, B.S. (2015): Distinguishing induced seismicity from natural seismicity in Ohio: demonstrating the utility of waveform template matching; Journal of Geophysical Research: Solid Earth, v. 120, no. 9, p. 6284–6296, URL <https://doi.org/10.1002/2015JB012265>.

Skoumal, R.J., Brudzinski, M.R. and Currie, B.S. (2018): Proximity of Precambrian basement affects the likelihood of induced seismicity in the Appalachian, Illinois, and Williston Basins, central and eastern United States; Geosphere, v. 14, no. 3, p. 1365–1379, URL <https://pubs.geoscienceworld.org/gsa/geosphere/article/14/3/1365/530435/Proximity-of-Precambrian-basement-affects-the> [April 2018].

Skoumal, R.J., Kaven, J.O. and Walter, J.I. (2019): Characterizing seismogenic fault structures in Oklahoma using a relocated template matched catalog; Seismological Research Letters, v. 90, no. 4, p. 1535-1543, URL <https://pubs.geoscienceworld.org/ssa/srl/article-abstract/90/4/1535/570858> [May 2019].

Smith, M.B. and Shlyapobersky, J.W. (2000): Basics of hydraulic fracturing; chapter *in* Reservoir Stimulation (3rd edition), M.J. Economides and K.G. Nolte (ed.), John Wiley and Sons, New York, New York, 856 p.

Stern, V.H., Schultz, R.J., Shen, L., Gu, Y.J. and Eaton, D.W. (2013). Alberta earthquake catalogue, version 1.0: September 2006 through December 2010; Alberta Energy Regulator, AER/AGS Open File Report 2013-15, p. 29, URL <https://ags.aer.ca/publication/ofr-2013-15> [September 2013].

Visser, R., Kao, H., Smith, B., Goerzen, C., Kontou, B., Dokht, R.M.H., Hutchinson, J., Tan, F. and Babaie Mahani, A. (2020): A comprehensive earthquake catalogue for the Fort St. John–Dawson Creek region, British Columbia, 2017–2018; Geological Survey of Canada, Open File 8718, 28 p., URL <https://doi.org/10.4095/326015>.

Visser, R., Smith, B., Kao, H., Babaie Mahani, A., Hutchinson, J. and McKay, J. (2017): A comprehensive earthquake catalogue for northeastern British Columbia and western Alberta, 2014–2016; Geological Survey of Canada, Open File, 8335, 28 p., URL <https://doi.org/10.4095/306292>.

Wozniakowska, P. and Eaton, D.W. (2020): Determination of factors controlling geological susceptibility to induced seismicity in the Montney Formation, northeastern British Columbia and northwestern Alberta, based on a machine-learning approach; *in* Geoscience BC Summary of Activities 2019: Energy and Water, Geoscience BC, Report 2020-

02, p. 19–26, URL <http://www.geosciencebc.com/i/pdf/SummaryofActivities2019/EW/Sch_PW_EW_SOA-2019.pdf> [February 2020].

Wrona, T., Pan, I., Gawthorpe, R.L. and Fossen, H. (2018): Seismic facies analysis using machine learning; Geophysics, v. 83, no. 5, p. O83-O95, URL <https://doi.org/10.1190/geo2017-0595.1>.

Zhang, H., Eaton, D., Rodriguez, G., and Jia, S.Q. (2019): Source-mechanism analysis and stress inversion for hydraulic-fracturing-induced event sequences near Fox Creek, Alberta; Bulletin of the Seismological Society of America, v. 109, no. 2, p. 636–651, URL <https://pubs.geoscienceworld.org/ssa/bssa/article-abstract/109/2/636/569194/Source-Mechanism-Analysis-and-Stress-Inversion-for?redirectedFrom=fulltext> [March 2019].